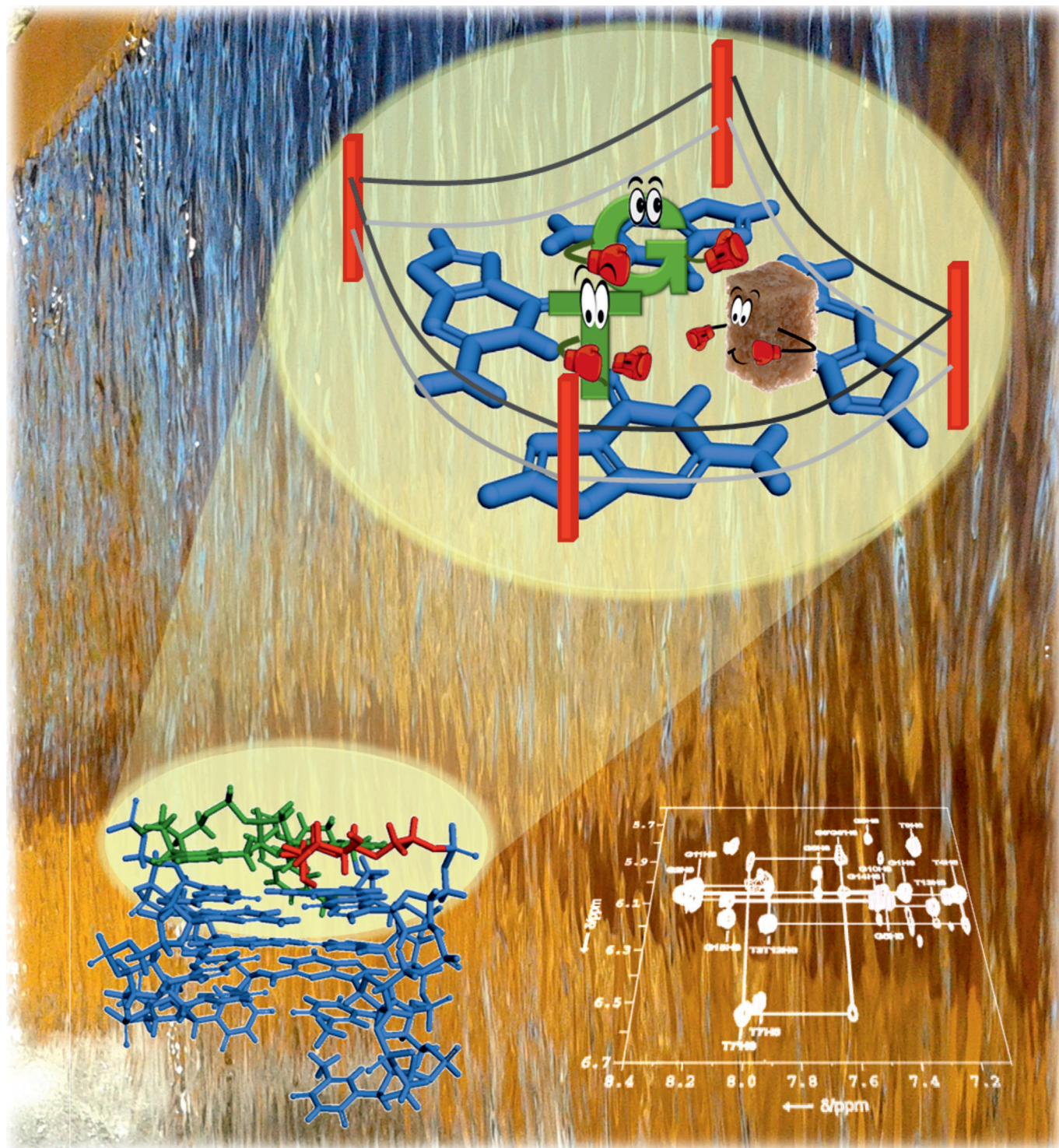


Carbohydrate–DNA Interactions at G-Quadruplexes: Folding and Stability Changes by Attaching Sugars at the 5'-End

Irene Gómez-Pinto,^[a] Empar Vengut-Climent,^[b] Ricardo Lucas,^[b] Anna Aviñó,^[c] Ramón Eritja,^[c] Carlos González,*^[a] and Juan Carlos Morales*^[b]



Abstract: Quadruplex DNA structures are attracting an enormous interest in many areas of chemistry, ranging from chemical biology, supramolecular chemistry to nanoscience. We have prepared carbohydrate–DNA conjugates containing the oligonucleotide sequences of G-quadruplexes (thrombin binding aptamer (TBA) and human telomere (TEL)), measured their thermal stability and studied their structure in

solution by using NMR and molecular dynamics. The solution structure of a fucose–TBA conjugate shows stacking interactions between the carbohydrate and the DNA G-tetrad in addition to hydrogen bonding and hydrophobic

Keywords: carbohydrates • DNA • G-quadruplexes • hydrogen bonds • molecular interactions • stacking

contacts. We have also shown that attaching carbohydrates at the 5'-end of a quadruplex telomeric sequence can alter its folding topology. These results suggest the possibility of modulating the folding of the G-quadruplex by linking carbohydrates and have clear implications in molecular recognition and the design of new G-quadruplex ligands.

Introduction

G-quadruplexes consist of a square arrangement of guanines (G-tetrad), stabilized by Hoogsteen hydrogen-bonding and by monovalent cations (especially potassium) coordinated in the center, located between two G-tetrads. The *in vivo* evidence of the existence of G-quadruplexes at telomeres^[1] and oncogene promoters,^[2] as well as their role in controlling different biological processes,^[3] have converted them in primary research targets for therapeutical applications.^[4] Consequently, a variety of ligands has been designed and prepared to bind G-quadruplexes as a new class of anticancer drugs. Some examples of quadruplex binders have been reported to bind through groove specific contacts of the quadruplex structure.^[5] However, most quadruplex ligands described to date use aromatic π -stacking as the main driving force for binding on the G-tetrad platform.^[6]

In addition, G-quadruplexes are a very attractive motif in the development of structural and functional supramolecular assemblies,^[7] and in DNA-based nanodevices.^[8] The possibility of modulating the physicochemical properties of a G-quadruplex by its conjugation to small molecules is also being explored, especially through attaching large aromatic groups.^[9]


We have used carbohydrate oligonucleotide conjugates (COCs) to study carbohydrate–DNA interactions in double helices adapting a dangling end DNA model system traditionally used to study π – π stacking interactions.^[10] The sugar moiety is attached to the 5'-end of the DNA sequence in our COCs. In previous work, we observed that natural highly polar carbohydrates stack onto the terminal DNA base pair of a duplex through CH/ π interactions.^[11] However, DNA stability is only increased when the sugars stack on C–G or G–C base pairs. If COCs contained permethylated carbohydrates, apolar versions of the natural sugars, a notable increase in double-stranded DNA stability was found in comparison with the natural polyhydroxylated mono- and disaccharide DNA conjugates. Moreover, these apolar carbohydrates are also capable of stabilizing duplexes with A–T or T–A terminal base-pairs.^[12] We hypothesized that the CH– π pseudo hydrogen-bonds in addition to the higher hydrophobicity imparted by the methyl groups are responsible for duplex stabilization.

Due to the relevance of the G-quadruplex DNA and RNA structures we decided to explore the possible carbohydrate–DNA interactions in a G-quadruplex context. Herein we describe the preparation of COCs containing the oligonucleotide sequence of a G-quadruplex and sugars attached to the 5'-end. The idea was to examine the possibility of carbohydrate interactions on top of the nearby G-tetrad and investigate how these contacts could affect quadruplex stability and structure. We have prepared COCs containing the thrombin-binding aptamer (TBA) and the human telomere (TEL) sequences in which the carbohydrates were covalently linked through an ethylene glycol spacer (Figure 1). Saccharides conjugated to a G-quadruplex-forming sequence (5'-TGGGAG) have been reported previously as anti-HIV agents.^[13] The TBA sequence (Figure 1A) was selected due to the detailed knowledge of its 3D structure^[14] and because of the high number of chemically modified TBA sequences (containing reverse natural bases,^[15] extra natural bases,^[16] modified bases,^[17] and unnatural nucleosides^[18]) and TBA conjugates (linked to small molecules^[19] and to nanostructures).^[20]

[a] Dr. I. Gómez-Pinto, Prof. Dr. C. González
Instituto de Química Física “Rocasolano”, CSIC
Serrano 119, 28006 Madrid (Spain)
E-mail: cgonzalez@iqfr.csic.es

[b] E. Vengut-Climent, Dr. R. Lucas, Dr. J. C. Morales
Department of Bioorganic Chemistry
Instituto de Investigaciones Químicas
CSIC–Universidad de Sevilla
Americo Vespucio 49, 41092 Sevilla (Spain)
E-mail: jcmorales@iiq.csic.es

[c] Dr. A. Aviñó, Prof. Dr. R. Eritja
Instituto de Investigación Biomédica de Barcelona
IQAC, CSIC, CIBER-BBN
Networking Centre on Bioengineering
Biomaterials and Nanomedicine
Baldiri Reixac 10, 08028 Barcelona (Spain)

 Supporting information for this article (including full experimental procedures and spectroscopic characterization data) is available on the WWW under <http://dx.doi.org/10.1002/chem.201203902>.

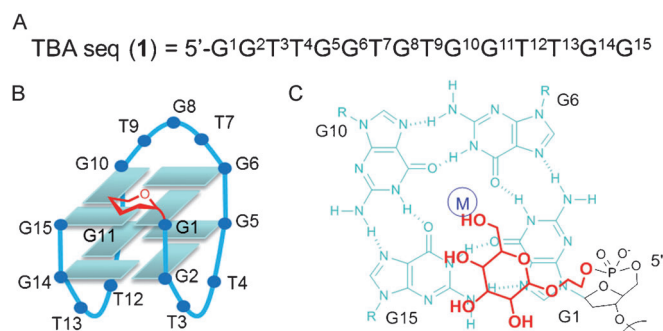


Figure 1. A) Sequence of the thrombin-binding aptamer (TBA). B) Schematic model of the carbohydrate-TBA conjugates. C) Enlarged top-view of monosaccharide-TBA conjugate.

Results and Discussion

The COCs were synthesized by using standard solid-phase oligonucleotide automatic synthesis. Mono- and disaccharides were covalently bound to the TBA sequence by using the corresponding carbohydrate phosphoramidite derivative (Figure 1 and Figure 2).^[11,21] β -D-glucose, β -D-galactose and

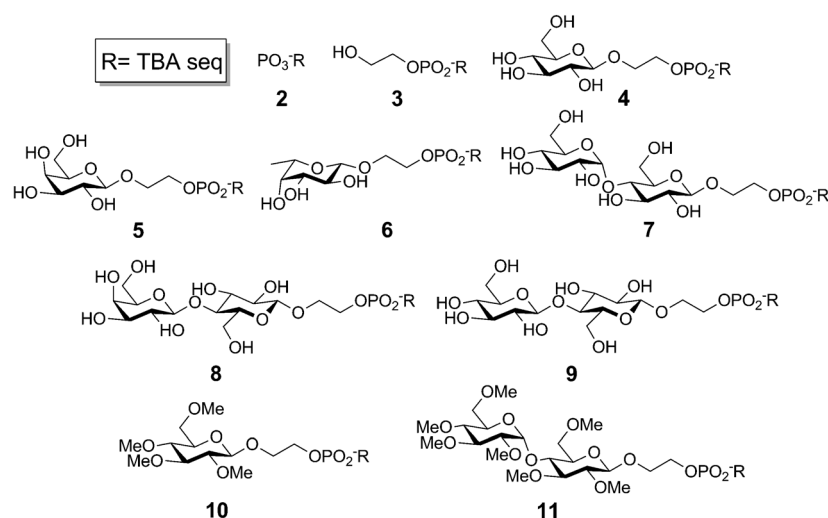


Figure 2. Carbohydrate-TBA conjugates and oligonucleotide controls prepared for this study.

β -L-fucose were the selected monosaccharides, whereas β -D-maltose, β -D-lactose and β -D-cellobiose were the chosen disaccharides. Also, two apolar sugars, permethylated glucose and maltose, were attached to the TBA sequence by using a similar synthetic strategy.^[12]

The thermal stability of the carbohydrate TBA conjugates was measured by UV-monitored thermal denaturation experiments in a pH 7.0 cacodylate buffer containing KCl (100 mM) (Table 1). All COCs containing natural carbohydrates (**4-9**) showed a lower thermal stability than the natural TBA (**1**). The reduction in T_m values ranges from 5.7 to 6.8°C. However, it is important to note that the addition of a phosphate group at the 5'-end of the TBA quadruplex

(compound **2**) provokes a destabilization of 4.5°C with respect to unmodified TBA **1**. Furthermore, when the spacer is attached to the TBA sequence (compound **3**) the decrease of T_m in comparison with TBA is 7.5°C. Therefore, compound **3** must be considered the proper control to evaluate the carbohydrate contribution to the thermal stability of the different conjugates. Thus, ΔT_m values of the natural carbohydrate TBA conjugates (**4-9**) with respect to the spacer-TBA conjugate (**3**) indicate an increase in stability between 0.7 and 1.8°C (see right column on Table 1). Thermodynamic analysis of the UV melting-curves were obtained by curve-fitting as described in the literature.^[22] Free energies confirmed the trend observed in the T_m values. Moreover, a greater enthalpic contribution to the stability of their folded structure is observed in all carbohydrate-TBA conjugates with respect to the spacer-TBA conjugate (**3**) and to natural TBA (**1**), which could be attributed to the new molecular interactions between carbohydrates and the G-quadruplex.

A similar scenario is observed when apolar carbohydrates are bound to the 5'-end of the TBA oligonucleotide. COCs containing permethylated glucose and maltose (**10** and **11**) also show a decrease in T_m values in comparison with TBA (4.7 and 10.1°C, respectively). Nevertheless, the TBA conjugate with the apolar version of glucose (**10**) is 2.8°C more stable than the control spacer-TBA (**3**) contributing to moderately improved TBA stability.

The addition of the natural and apolar sugars to the conjugate **3** is able to recover, to some extent, the TBA G-quadruplex stability. These results indicate that favorable carbohydrate-DNA interactions are taking place.

We also measured the thermal stability of oligonucleotide TBA sequences with an extra base at the 5'-end (thymidine, sequence **12** and adenine, sequence **13**). A decrease in T_m value was observed for both sequences (6.0 and 6.3°C, respectively)

with respect to the unmodified TBA (**1**). Comparable results were obtained by Smirnov et al.;^[23] these values are similar to those obtained for COCs with the natural carbohydrates and a similar behavior could be envisioned. It is important to note that here the "spacer" of the natural aromatic base is deoxyribose, which is conformationally more restricted than ethylene glycol, the spacer used for the mono- and disaccharide TBA conjugates.

To confirm that the observed increased stability in COCs is due to carbohydrate-G-tetrad interaction, the structure of TBA-carbohydrate conjugates containing two mono- and three disaccharides (compounds **5**, **6**, **7**, **8**, and **9**) was studied by NMR spectroscopy, circular dichroism (CD), and gel

Table 1. Melting temperatures T_m values ($^{\circ}\text{C}$) for the carbohydrate–oligonucleotide conjugates containing the thrombin-binding aptamer sequence and the corresponding oligonucleotide controls.^[a]

5'-X-GGTTGGTGTGGTTGG	T_m [$^{\circ}\text{C}$]	ΔT_m [$^{\circ}\text{C}$] ^[b]	ΔT_m^* [$^{\circ}\text{C}$] ^[c]	$-\Delta S^{\circ}$ [kcal mol^{-1}]	$-\Delta H^{\circ}$ [kcal mol^{-1}]	ΔG_{37}° [kcal mol^{-1}]	$\Delta\Delta G_{37}^{\circ}$ [kcal mol^{-1}] ^[d]	$\Delta\Delta G_{37}^{\circ*}$ [kcal mol^{-1}] ^[e]
(none)	1	48.2 ± 0.5	–	–7.5	117.5 ± 2	37.7 ± 0.5	–2.8	–
PO_3^-	2	43.7 ± 0.2	–4.5	–3.0	134.1 ± 2	42.3 ± 0.5	–2.3	0.5
HO-C2-OPO_2^- ^[f]	3	40.7 ± 0.2	–7.5	–	119.8 ± 1	37.5 ± 0.4	–1.8	1.0
$\beta\text{-D-glucose-C2-OPO}_2^-$ ^[f]	4	42.5 ± 0.2	–5.7	+1.8	132.3 ± 1	41.7 ± 0.4	–2.2	0.6
$\beta\text{-D-galactose-C2-OPO}_2^-$ ^[f]	5	41.4 ± 0.2	–6.8	+0.7	135.1 ± 2	42.3 ± 0.5	–2.0	0.8
$\beta\text{-L-fucose-C2-OPO}_2^-$ ^[f]	6	42.3 ± 0.2	–5.9	+1.6	135.7 ± 2	42.6 ± 0.5	–2.2	0.6
$\beta\text{-D-maltose-C2-OPO}_2^-$ ^[f]	7	41.7 ± 0.2	–6.5	+1.0	133.7 ± 2	42.0 ± 0.5	–2.1	0.7
$\beta\text{-D-lactose-C2-OPO}_2^-$ ^[f]	8	41.5 ± 0.3	–6.7	+0.8	139.7 ± 2	43.8 ± 0.7	–2.2	0.6
$\beta\text{-D-cellobiose-C2-OPO}_2^-$ ^[f]	9	41.8 ± 0.3	–6.4	+1.1	136.9 ± 2	42.9 ± 0.6	–2.1	0.7
$\beta\text{-D-glucose(Me)-C2-OPO}_2^-$ ^[f]	10	43.5 ± 0.7	–4.7	+2.8	134.1 ± 1	42.4 ± 0.5	–2.4	0.4
$\beta\text{-D-maltose(Me)-C2-OPO}_2^-$ ^[f]	11	38.1 ± 0.4	–10.1	–1.6	127.2 ± 2	39.7 ± 0.5	–1.8	1.0
2'-deoxythymidine-OPO ₂ [–]	12	42.2 ± 0.1	–6.0	+1.5	141.5 ± 3	44.4 ± 0.8	–2.2	0.6
2'-deoxyadenosine-OPO ₂ [–]	13	41.9 ± 0.1	–6.3	+1.2	139.2 ± 2	43.8 ± 0.6	–2.3	0.5

[a] Buffer: Na-cacodylate (10 mM), KCl (100 mM), pH 7.0; T_m values are the average of three experiments measured at 5 μM . [b] $\Delta T_m = T_m$ (5'-modified TBA sequence) – T_m (TBA control sequence). [c] $\Delta T_m^* = T_m$ (5'-modified TBA sequence) – T_m (5'-spacer-OPO₂[–]-TBA sequence). [d] $\Delta\Delta G_{37}^{\circ} = \Delta G$ (5'-modified TBA sequence) – ΔG (TBA control sequence). [e] $\Delta\Delta G_{37}^{\circ*} = \Delta G$ (5'-modified TBA sequence) – ΔG (5'-spacer-OPO₂[–]-TBA sequence). [f] C2 represents $-\text{CH}_2-\text{CH}_2-$.

electrophoresis. CD spectra clearly show that all conjugates adopt antiparallel G-quadruplex structures (see Figure S1 in the Supporting Information). Gel electrophoresis experiments conducted under non-denaturing conditions show single bands for monosaccharide–TBA conjugates, running as the native TBA. However, two bands are observed for the disaccharide–TBA conjugates (Figure S2 in the Supporting Information). Since the melting temperatures of these conjugates do not depend on oligonucleotide concentration (Table S1 in the Supporting Information), we conclude that the two bands observed in the gels correspond to two monomeric species with different conformations.

The imino proton region of the NMR spectra clearly indicates that all conjugates adopt a quadruplex structure with two guanine tetrads (Figure S3 in the Supporting Information). Exchangeable proton signals could be assigned on the basis of the strong similarity between the spectra of the conjugates and the unmodified aptamer. Assignment of most non-exchangeable protons could be carried out following standard bidimensional techniques, and were confirmed with previously reported assignment of native TBA (see Figures 3 and 4 and the Supporting Information for assignment tables).

In the case of the disaccharide conjugates, spectral assignment was complicated due to the presence of additional spin-systems. After sequential assignment, we concluded that these systems correspond to two species, affecting protons in residues G6, T7, and G8 (see Figure 3), being both species in slow equilibrium on the NMR timescale. The chemical shifts of one of the conformations are almost coincident with those of the native aptamer.

This effect is not observed in the monosaccharide–TBA conjugates, in which single species are observed. The different behavior between mono- and disaccharide conjugates is consistent with the non-denaturing gel experiments. Chemical shift differences between equivalent protons in modified- and unmodified TBA are shown in Figure S4 (the

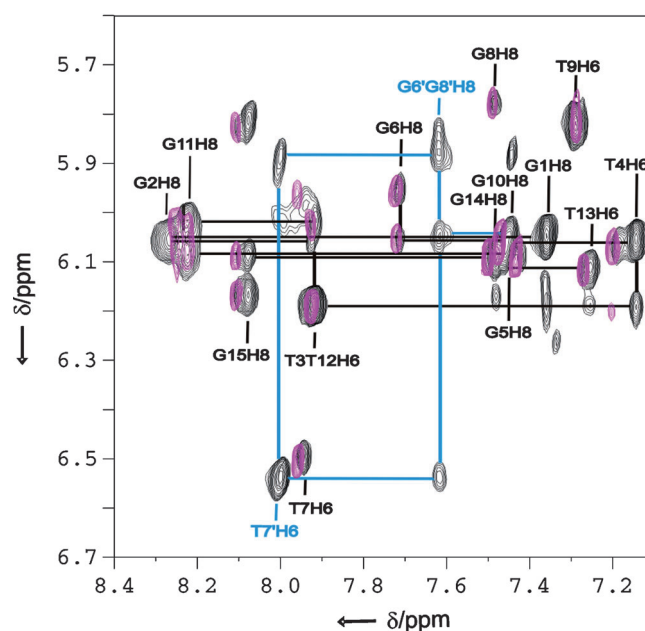


Figure 3. Region of the NOESY spectra of the maltose–TBA conjugate (7) superimposed onto the native TBA (1, pink) spectra. Sequential assignment pathways show the two different species for residues G6, T7 and G8 (labeled in different colors).

Supporting Information). Most protons in COCs exhibit very similar chemical shifts to the natural TBA except those in residue G1 and in the neighborhood of the TGT loop (mainly, protons in residues G6, T7, and G8). Interestingly, the profile of chemical shift differences is very similar in all the conjugates.

NOE data also indicate that all conjugates maintain a similar structure as the native TBA. Exchangeable NOE patterns are consistent with formation of two G-tetrads. The strong intensities of intraresidue NOE cross-peaks between guanine H8 and H1' protons confirmed the *syn* conforma-

tion for the glycosidic angle of G1, G5, G10, and G14. Stacking of the lateral loop thymines, T4 and T13, on top of the adjacent guanines, G2 and G11, is corroborated by several strong NOEs. However, some differences in NOE cross-peaks are observed in the TGT loop suggesting that the carbohydrate affects its structure and alters the interaction of residues G8 and T9 with the nearby tetrad (G1:G6:G10:G15; see Figure 4 and Table S2 in the Supporting Information).

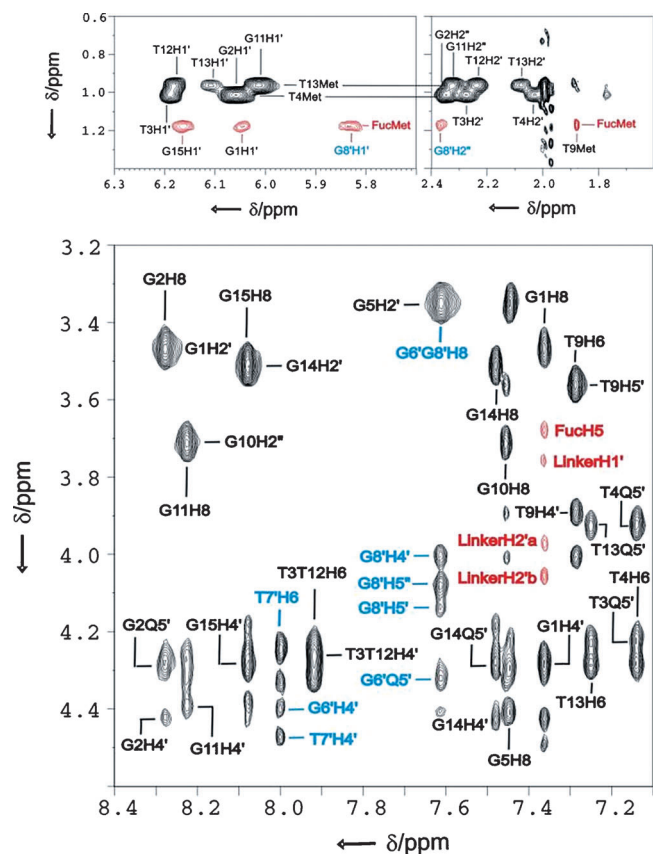


Figure 4. Regions of the NOESY experiments of fucose-TBA conjugate (6). Contour plots of the carbohydrate–DNA NOEs are shown in red.

Most interestingly, several carbohydrate–DNA NOEs could be detected in all conjugates. The number of these NOEs is particularly high in the case of conjugate 6 (fucose–TBA), most probably due to the presence of a methyl group in this carbohydrate; this resonance is easily identified and does not overlap with other signals of the conjugate (see Figure 4, top).

The solution structure of conjugate 6 was determined on the basis of experimental NOE constraints. Restrained molecular-dynamics calculations were carried out with the AMBER package as explained in the Methods section in the Supporting Information. A total of 142 distance constraints (10 between carbohydrate and DNA) were used in the calculation (Table S2, the Supporting Information). Structures were deposited in the Protein Data Bank (2lyg).

As shown in Figure 5, the resulting structures are well-defined. The solution structure of the fucose–TBA conjugate resembles the general fold of the unmodified aptamer. The main differences are in the TGT loop-region in which the fucose moiety displaces the nucleobases of residues G8 and T9 and stacks on top of G1 and G15 (see Figure 5, bottom). In fact, fucose interaction with the guanine tetrad seems to occur by an induced-fit mechanism. In addition to the stacking interaction with the adjacent tetrad, fucose O5 is at a hydrogen bond distance of one amino proton of G8 (see Figure 6). Also, a favorable hydrophobic interaction occurs between fucose and T9 methyl groups (Figure 6). The T7 base tends to insert into the quadruplex groove. The carbohydrate maintains the usual 4C_1 chair conformation.

The structure of the conjugate 6 is totally consistent with the observed NOEs and the profiles of chemical shift differences between this conjugate and the native aptamer. Chemical shifts are very sensitive to structural variations. Therefore, the strong similarity between DNA proton resonances in the two monosaccharide–DNA conjugates implies that fucose–TBA and galactose–TBA adopt very similar conformations (see Figure S5 in the Supporting Information). Although in the latter the number of carbohydrate–DNA NOEs is lower, this is not due to a different conformation of the galactose in the conjugate, but to the lack of the fucose methyl-group that facilitates the detection of carbohydrate–DNA NOEs.

Inspection of the structure of fucose–TBA shows that the site occupied by the fucose sugar cannot be easily occupied by a disaccharide without further disruption of the TGT loop (see Figure 5). Most probably, this is the reason of the two species observed in the NMR spectra of the disaccharide conjugates, and confirmed by electrophoretic gels. 1H chemical shifts and NOEs suggest that in one species the disaccharide interacts with the G-tetrad disrupting the TGT loop, and in the other, the TGT loop adopts a native-like conformation with the disaccharide mainly disordered (Figure 7). Presumably, this second species has a different electrophoretic mobility (see Figure S2 in the Supporting Information). At the same time, this equilibrium must be affecting the stability of the carbohydrate–TBA conjugate.

It is worth mentioning that the disaccharide–TBA conjugates are not more stable than the monosaccharide–TBA conjugates, as observed in the case of sugar-capping DNA duplexes.^[11–12] The stabilization conferred to the TBA by the different carbohydrates is more difficult to interpret than in the case of carbohydrates stacking at the terminal base of double helices. In the latter, the increase in thermal stability is a direct measurement of a favorable interaction of the carbohydrate with the terminal base pair. However, in TBA conjugates the carbohydrate G-tetrad interaction competes with native nucleobase π -stacking interactions. This event is difficult to circumvent because G-tetrads are rarely exposed to the solvent. In fact, the capping interactions in the terminal G-tetrads affect dramatically the folding topology of the quadruplex.

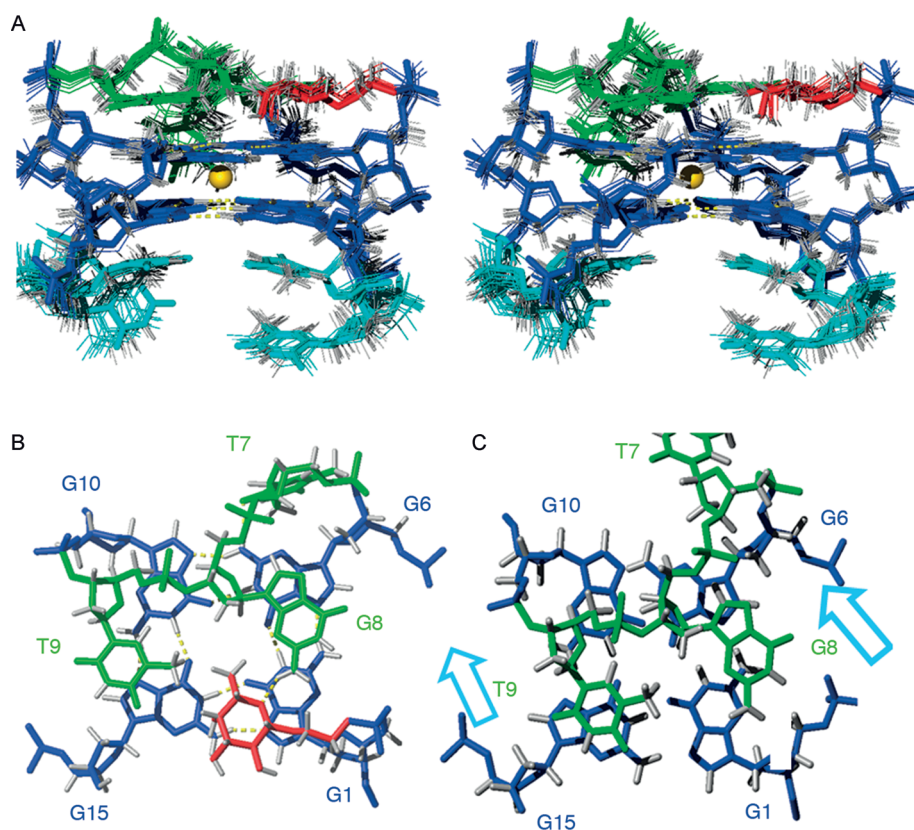


Figure 5. A) Stereoview of the superposition of 10 refined structures of the fucose–TBA, conjugate **6**. The average structure is shown in bold bonds. B) Top view of the fucose–TBA conjugate **6**. C) Top view of the native TBA G-quadruplex **1** (arrows indicate the direction where G8 and T9 move in the fucose–TBA conjugate **6**). The fucose moiety is shown in red, guanine core in blue, –TT– lateral loops in cyan, and the –TGT– loop in green.

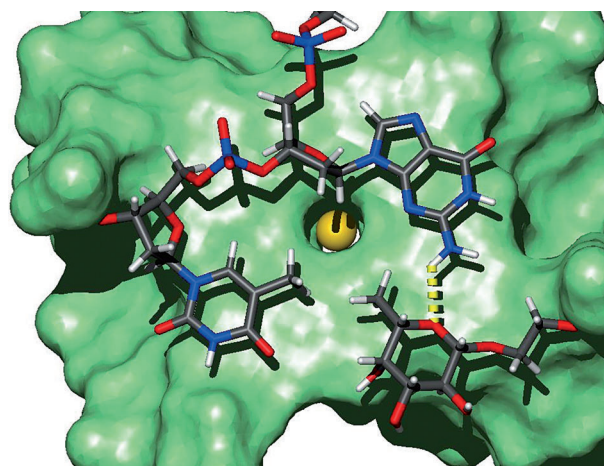


Figure 6. Detail on the structure of the fucose–TBA conjugate **6**. Contacts of fucose with the bases of G8 and T9 in the TGT loop of the G-quadruplex can be observed (methyl–methyl interactions and a hydrogen bond shown in yellow).

Interfering with capping interactions by conjugating carbohydrates makes it possible to modulate G-quadruplex folding, since the particular topology adopted by a G-rich oligonucleotide depends strongly on capping interactions be-

tween terminal G-tetrads and nucleotides in the loops. In many cases, terminal residues are also involved in these interactions, as observed in human telomeric sequences. As a proof of concept, we have explored the effect of substituting the 5'-terminal thymine of the oligonucleotide 5'-TAGGGT-TAGGGT-3' (TEL) with a carbohydrate. TEL folds as a G-quadruplex containing two repeats of the human telomeric sequence, and its structure has been studied by NMR spectroscopy and X-ray crystallography. In the crystallographic structure TEL forms a dimeric parallel propeller-like quadruplex.^[24] However, in solution, TEL exists in an equilibrium between dimeric parallel and antiparallel structures, being the latter predominant in Na⁺ buffer.^[25]

As it can be observed in Figure 8, the NMR spectra of TEL and β -D-glucose-C2-OPO₂⁻-AGGGTTAGGGT **14** are dramatically different. As

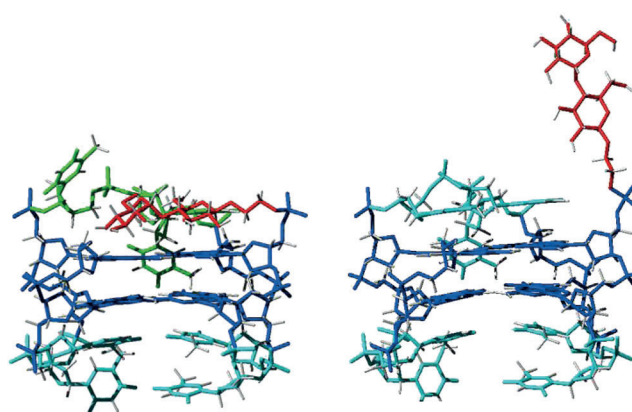


Figure 7. Side view of the two possible conformations of maltose–TBA conjugate **7**: Left: maltose stacked on the G-tetrad with T9 shifted; right: maltose pointing to the bulk aqueous solution with T9 and G8 stacked on the G-tetrad.

previously reported, the TEL spectra exhibit many broad imino signals, indicating the presence of multiple conformations. A similar complexity is observed in the control spacer-OPO₂⁻-AGGGTTAGGGT conjugate **15** (see Figure S9 in the Supporting Information).

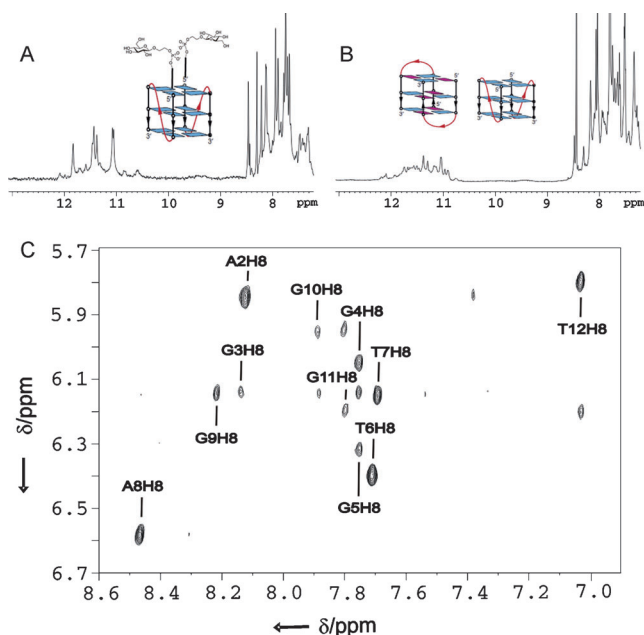


Figure 8. Imino region of the NMR spectra of A) **14** and B) TEL and schemes of the two species coexistent in solution; C) H1'-aromatic region of the NOESY spectra of **14** in D₂O ($\tau_m = 300$ ms) (Experimental conditions: oligo concentration = 1 mM, potassium phosphate buffer (10 mM), pH 7, $T = 5^\circ\text{C}$).

However, the imino region of the NMR spectra of the carbohydrate–TEL conjugate **14** shows six sharp signals, indicating clearly the presence of a single conformation. The two-dimensional spectra of **14** shown in Figure 8 indicates that all guanines are in an *anti*-conformation. These data are consistent with the formation of a parallel symmetric quadruplex. A complete structural determination of this and other COCs containing telomeric sequences is in progress in our laboratories and will be reported in due time. With the present data we can already conclude that substitution of the 5'-terminal thymine by glucose alters the equilibrium between different species, promoting the formation of a stable parallel quadruplex (see Figure 8).

Conclusion

Our studies on sugar–DNA conjugates show that favorable carbohydrate–DNA interactions occur in a G-quadruplex structural context as we have observed in the case of TBA. Carbohydrates stack on top of guanine tetrads, and also interact with loop DNA bases through hydrogen bonding or hydrophobic contacts when they are available (like the interaction between fucose and thymine methyl groups in the fucose–TBA conjugate).

Our results have implications in the design of new G-quadruplex ligands. Until now only aromatic compounds binding through π – π stacking on the guanine tetrad or through van der Waals contacts with the grooves of the G-quadruplex structures have been reported. Our results

engage the possibility of developing carbohydrate-based ligands that could bind through CH– π noncovalent forces together with other molecular interactions.

Finally, we have also shown that by conjugating carbohydrates at the 5'-end of G-quadruplex structures, we can alter their folding topology. The success of the modulation is based on manipulating the interaction between the terminal G-tetrads and other residues. The intrinsic versatility of carbohydrates introduces the possibility of modulating G-quadruplex systems in nanomaterials and biomedical applications.

Acknowledgements

We thank the MICINN (grants CTQ2009–13705, CTQ2010–20451, CTQ2010–21567-C02-02), EU COST project MP0802, Generalitat de Catalunya (2009/SGR/208), and Instituto de Salud Carlos III (CIBER-BNN, CB06 01 0019) for financial support. IGP and RL thank CSIC for a JAE contract. EVC thanks the Ministry of Education for an FPU doctoral fellowship.

- [1] K. Paeschke, T. Simonsson, J. Postberg, D. Rhodes, H. J. Lipps, *Nat Struct Mol Biol* **2005**, *12*, 847–854.
- [2] a) T. A. Brooks, L. H. Hurley, *Nat Rev Cancer* **2009**, *9*, 849–861; b) D. Sun, K. Guo, Y.-J. Shin, *Nucleic Acids Res.* **2011**, *39*, 1256–1265.
- [3] a) S. Balasubramanian, L. H. Hurley, S. Neidle, *Nat Rev Drug Discov* **2011**, *10*, 261–275; b) H. J. Lipps, D. Rhodes, *Trends Cell Biol.* **2009**, *19*, 414–422.
- [4] a) G. W. Collie, G. N. Parkinson, *Chem. Lett. Chem. Soc Rev* **2011**, *40*, 5867–5892; b) Y. Qin, L. H. Hurley, *Biochimie* **2008**, *90*, 1149–1171.
- [5] S. Cosconati, L. Marinelli, R. Trotta, A. Virno, S. De Tito, R. Romagnoli, B. Pagano, V. Limongelli, C. Giancola, P. G. Baraldi, L. Mayol, E. Novellino, A. Randazzo, *J Am Chem. Soc* **2010**, *132*, 6425–6433.
- [6] a) S. M. Haider, S. Neidle, G. N. Parkinson, *Biochimie* **2011**, *93*, 1239–1251; b) S. Neidle, *FEBS J.* **2010**, *277*, 1118–1125.
- [7] M. Nikan, J. C. Sherman, *Angew. Chem. Int. Ed.* **2008**, *47*, 4900–4902.
- [8] a) H.-M. So, K. Won, Y. H. Kim, B.-K. Kim, B. H. Ryu, P. S. Na, H. Kim, J.-O. Lee, *J Am Chem. Soc* **2005**, *127*, 11906–11907; b) C.-L. Hsu, H.-T. Chang, C.-T. Chen, S.-C. Wei, Y.-C. Shiang, C.-C. Huang, *Chem. Eur. J.* **2011**, *17*, 10994–11000.
- [9] a) F. D. Lewis, Y. Wu, L. Zhang, *Chem. Commun.* **2004**, 636–637; b) J. Jayawickramarajah, D. M. Tagore, L. K. Tsou, A. D. Hamilton, *Angew. Chem. Int. Ed.* **2007**, *46*, 7583–7586.
- [10] a) M. Senior, R. A. Jones, K. J. Breslauer, *Biochemistry* **1988**, *27*, 3879–3885; b) K. M. Guckian, B. A. Schweitzer, R. X. F. Ren, C. J. Sheils, D. C. Tahmassebi, E. T. Kool, *J. Am. Chem. Soc.* **2000**, *122*, 2213–2222; c) Z. Dogan, R. Paulini, J. A. Rojas Stutz, S. Narayanan, C. Richert, *J Am Chem. Soc* **2004**, *126*, 4762–4763.
- [11] R. Lucas, I. Gómez-Pinto, A. Aviñó, J. J. Reina, R. Eritja, C. González, J. C. Morales, *J Am Chem. Soc* **2011**, *133*, 1909–1916.
- [12] R. Lucas, E. Vengut-Climent, I. Gómez-Pinto, A. Aviñó, R. Eritja, C. González, J. C. Morales, *Chem. Commun.* **2012**, *48*, 2991–2993.
- [13] J. D'Onofrio, L. Petraccone, L. Martino, G. Di Fabio, A. Iadonisi, J. Balzarini, C. Giancola, D. Montesarchio, *Bioconjugate Chem.* **2008**, *19*, 607–616.
- [14] a) R. F. Macaya, P. Schultze, F. W. Smith, J. A. Roe, J. Feigon, *Proc Natl Acad Sci USA* **1993**, *90*, 3745–3749; b) K. Y. Wang, S. McCurdy, R. G. Shea, S. Swaminathan, P. H. Bolton, *Biochemistry* **1993**, *32*, 1899–1904; c) K. Padmanabhan, K. P. Padmanabhan, J. D. Ferrara,

- J. E. Sadler, A. Tulinsky, *J Biol Chem.* **1993**, *268*, 17651–17654; d) J. A. Kelly, J. Feigon, T. O. Yeates, *J Mol Biol* **1996**, *256*, 417–422.
- [15] L. Martino, A. Virno, A. Randazzo, A. Virgilio, V. Esposito, C. Giancola, M. Bucci, G. Cirino, L. Mayol, *Nucleic Acids Res.* **2006**, *34*, 6653–6662.
- [16] A. De Rache, I. Kejnovska, M. Vorlickova, C. Buess-Herman, *Chem. Eur. J.* **2012**, *18*, 4392–4400.
- [17] a) S. R. Nallagatla, B. Heuberger, A. Haque, C. Switzer, *J Comb Chem.* **2009**, *11*, 364–369; b) J. Gros, A. Aviñó, J. Lopez de La Osa, C. Gonzalez, L. Lacroix, A. Perez, M. Orozco, R. Eritja, J. L. Mergny, *Chem. Commun.* **2008**, 2926–2928; c) S. Ogasawara, M. Maeda, *Angew. Chem. Int. Ed.* **2009**, *48*, 6671–6674.
- [18] a) T. Coppola, M. Varra, G. Oliviero, A. Galeone, G. D’Isa, L. Mayol, E. Morelli, M. R. Bucci, V. Vellecco, G. Cirino, N. Borbone, *Bioorg. Med. Chem.* **2008**, *16*, 8244–8253; b) Y. Kasahara, S. Kitadume, K. Morihira, M. Kuwahara, H. Ozaki, H. Sawai, T. Imanishi, S. Obika, *Bioorg. Med. Chem. Lett.* **2010**, *20*, 1626–1629; c) C. G. Peng, M. J. Damha, *Nucleic Acids Res.* **2007**, *35*, 4977–4988; d) A. Pasternak, F. J. Hernandez, L. M. Rasmussen, B. Vester, J. Wengel, *Nucleic Acids Res.* **2011**, *39*, 1155–1164; e) H. Saneyoshi, S. Mazzini, A. Aviñó, G. Portella, C. Gonzalez, M. Orozco, V. E. Marquez, R. Eritja, *Nucleic Acids Res.* **2009**, *37*, 5589–5601.
- [19] a) A. Aviñó, S. Mazzini, R. Ferreira, R. Eritja, *Bioorg. Med. Chem.* **2010**, *18*, 7348–7356; b) S. Nagatoishi, T. Nojima, B. Juskowiak, S. Takenaka, *Angew. Chem. Int. Ed.* **2005**, *44*, 5067–5070.
- [20] a) Y. Wang, F. Yang, X. Yang, *Biosens. Bioelectron.* **2010**, *25*, 1994–1998; b) H. de Puig, S. Federici, S. H. Baxamusa, P. Bergese, K. Hamad-Schifferli, *Small* **2011**; c) Y. C. Shiang, C. L. Hsu, C. C. Huang, H. T. Chang, *Angew. Chem. Int. Ed.* **2011**, *50*, 7660–7665.
- [21] J. C. Morales, J. J. Reina, I. Díaz, A. Aviñó, P. M. Nieto, R. Eritja, *Chem. Eur. J.* **2008**, *14*, 7828–7835.
- [22] J. D. Puglisi, I. Tinoco, Jr., *Methods Enzymol* **1989**, *180*, 304–325.
- [23] I. Smirnov, R. H. Shafer, *Biochemistry* **2000**, *39*, 1462–1468.
- [24] G. N. Parkinson, M. P. Lee, S. Neidle, *Nature* **2002**, *417*, 876–880.
- [25] A. T. Phan, D. J. Patel, *J Am Chem. Soc* **2003**, *125*, 15021–15027.

Received: October 31, 2012
Published online: January 11, 2013